Journal of the European Ceramic Society **16** (1996) 169–175

0955-2219(95)00150-6
0955-2219/96/$15.00

Infra-red Spectroscopic Investigation in the Mullite Field of Composition: $Al_2(Al_{2+2x}Si_{2-2x})O_{10-x}$ with $0{\cdot}55 > x > 0{\cdot}25$

C. H. Rüscher, G. Schrader & M. Götte

Institut für Mineralogie der Universität Hannover und SFB 173, Welfengarten 1, 30167 Hannover, Germany

(Accepted 22 July 1995)

Abstract

The infra-red absorption of 2 : 1 and 3 : 2 mullites, and a series of heat-treated mullite starting materials of nominal composition $3Al_2O_3{\cdot}2SiO_2$ prepared by the sol–gel process, are investigated in the spectral range 400–1400 cm^{-1} using the KBr powder method. It is shown that the intensity variation of the absorption band in the spectral range 1100–1200 cm^{-1} provides a useful empirical scale for the determination of mullite compositions. This absorption feature exhibits the superposition of three peaks, which are related to vibrations of the mullite specific tetrahedral units $[SiO_4]$, $[AlO_4]$ and $[Al^*O_4]$ with frequency maxima at about 1165, 1130 and 1108 cm^{-1}, respectively.

1 Introduction

Mullite, $Al_2(Al_{2+2x}Si_{2-2x})O_{10-x}V_x$, is one of the most important ceramic products. The stability field of mullite depends on the ability to accommodate oxygen vacancies (V), which is commonly described by the exchange reaction $2Si^{4+} + O^{2-}$ to $2Al^{3+} + V$. Cameron[1,2] put forward the view of a solid solution in the stability field of mullite. The silica-rich limit has been observed for $x \approx 0{\cdot}17$, possessing a hypothetical miscibility gap to the structurally closely related mineral sillimanite of $x = 0$ composition. This relationship can be seen by assuming an Al–Si disorder on the tetrahedral sites of the sillimanite structure. The field of solid solution, on the other hand, is implied by the incorporation of oxygen vacancies and the development of the lattice constants on x. The **a**-lattice parameter of the orthorhombic unit cell (*Pbam*) of mullite increases linearly from about $a = 0{\cdot}754$ nm for so-called 3 : 2 'ideal'[1] sinter mullite ($x = 0{\cdot}25$) to $a = 0{\cdot}757$ nm for 2 : 1 melt mullite ($x = 0{\cdot}4$). Along this route of compositions the **c** and **b** lattice parameters also vary systematically; however, more smoothly compared with the **a** values ($b \approx 0{\cdot}768$–$0{\cdot}769$ nm; $c \approx 0{\cdot}2886$–$0{\cdot}289$ nm). The linear increase of the **a** lattice parameter still holds towards higher x values, while the **b** parameter drops down slightly and shows $a = b \approx 0{\cdot}766$ nm for $x \approx 0{\cdot}67$[1,2] (see also Ref. 3 and references therein). Thus, the empirical rule of the development of the lattice parameters (commonly the **a** lattice constant) can be used for an estimation of the composition of mullite ceramics and powders using X-ray diffraction techniques, as has often been reported (compare Ref. 3).

Another potential technique to estimate the composition of mullite has also been suggested by Cameron.[1] By using KBr diluted pressed pellets of various mullites, Cameron[1] observed a systematic change in the line profile of the infra-red absorption in the spectral range 1100 to 1200 cm^{-1} as a function of Al_2O_3 content. On the other hand, the infra-red technique has been used by various authors to investigate mullite crystallization (compare, e.g., Ref. 4) without, however, exploring the possibility of characterization of the mullite composition in any detail, an oversight which will be addressed in this study.

It is proposed here to follow the crystallization of mullite from base non-crystalline mullites of composition $x = 0{\cdot}25$ (3 : 2 mullite), prepared by the sol–gel process with different methods of hydrolysis. The synthesis and structural characterization of these materials (precursor material) have been given in detail previously,[5,6] and it has been shown that so-called types I, II and III precursors show crystallization of mullite at 900, 1200 and 1200°C, respectively. It is known that type I precursors show a gradual change from initial mullite with high Al_2O_3 content to mullite of bulk composition $x = 0{\cdot}25$ (above ~ 1400°C), similar to observations reported by Okada and Otsuka[7] (see also Refs 3, 5, 6, 8). Type II and III precursors, on the other hand, form γ-Al_2O_3 prior

to the crystallization of mullite.[3,5,8,9] Thus, by investigating these crystallization processes, information on the applicability of the KBr infra-red spectroscopic technique to the determination of mullite compositions can be expected.

It may be noted that MacKenzie[10] was the first to obtain an assignment of infra-red frequencies of a mullite of composition $x = 0{\cdot}25$ (3:2 mullite), using simplified structural models in comparison with a KBr powder spectrum. MacKenzie[10] could resolve about eight oscillator frequencies. However, it has been shown recently,[11] on the basis of single crystal infra-red investigations of mullite of composition $x = 0{\cdot}4$ (2:1 mullite), that the spectra show strong anisotropy and that 14, 14 and nine oscillator frequencies can be resolved for the polarizations $E||a$, $E||b$ and $E||c$, respectively. The absorption bands are all close together, distributed mainly in the spectral range 300 to 1000 cm^{-1} and 1100 to 1200 cm^{-1}. This indeed creates serious problems in achieving any accurate determination of oscillator frequencies from KBr powder spectra, a point which will also be discussed here.

2 Experimental

The non-crystalline mullite base materials used in this study were kindly provided by Schneider and co-workers (DLR, Germany). These materials were synthesized starting from tetraethyl orthosilicate (TEOS) and aluminium-sec-butylate (Al–O–Bu). The educts were formulated with the stoichiometric composition 3 Al_2O_3:2 SiO_2. After different routes of hydrolysis (type I: low water content, slow hydrolysis; types II and III: high water content and fast hydrolysis with pH values of >10 and <10, respectively), the materials were calcined at 350°C for preservation. Details of the preparation techniques and further characterization of the precursors are given by Schneider and co-workers.[5,6] A series of samples was prepared from each batch, these samples being subjected to further heat treatments at temperatures between 800 and 1650°C. Each sample (100 mg) was placed in a Pt crucible, heated up to its defined burning temperature at 300°C min^{-1} and quenched by removing the sample from the furnace. The holding time at the burning temperature was 15 h in each case.

The products were investigated by standard X-ray powder methods (Guinier camera) and by infra-red (IR) spectroscopic means (Bruker FTIR IFS88). For the IR measurements the samples were ground to an average particle size of ~1 μm and diluted with KBr (sample:KBr = 1:250 wt%; total weight ≈ 1 g). From these mixtures 250 mg were taken and pressed to obtain clear discs for the measurements. All spectra are plotted in absorption units according to $-\ln(I/I_0)$. I, I_0 = transmitted intensity of the sample plus KBr and pure KBr discs, respectively. For comparison, mullite samples of known 3:2 composition (extracted from sintered mullites) and 2:1 mullites (extracted from melt mullites) were investigated using the same route.

3 Results

KBr powder spectra of pure mullites of known composition $x = 0{\cdot}25$ ($3Al_2O_3{\cdot}2SiO_2$) and $x = 0{\cdot}4$ ($2Al_2O_3{\cdot}SiO_2$) are shown in Fig 1. Although the line shapes of the spectra look similar, there are characteristic distinctions. The main features observed in the spectrum of the 2:1 mullite are marked by dotted lines. Their vertical extensions are shown for better comparison with the spectrum of the 3:2 mullite. Below about 500 cm^{-1} the spectral line profiles indicate slight differences that are, however, hard to resolve systematically because of experimental difficulties. The peak maximum at ~545 cm^{-1} in the 2:1 spectrum appears to be shifted to ~575 cm^{-1} in the 3:2 spectrum. There is a sharper peak structure at ~740 cm^{-1} in the 3:2 spectrum compared with the 2:1 one. This feature could be related to the difference in intensity of the peak structures at ~810 cm^{-1} and 895 cm^{-1}. The most prominent spectral difference is observed in the absorption line profile in the spectral range 1100 to 1200 cm^{-1}. The spectrum of the 3:2 mullite is in sufficient agreement with the KBr powder spectrum of a 3:2 mullite reported by MacKenzie.[10] MacKenzie[10] related the peak structure in the spectral range 1100 to 1200 cm^{-1}

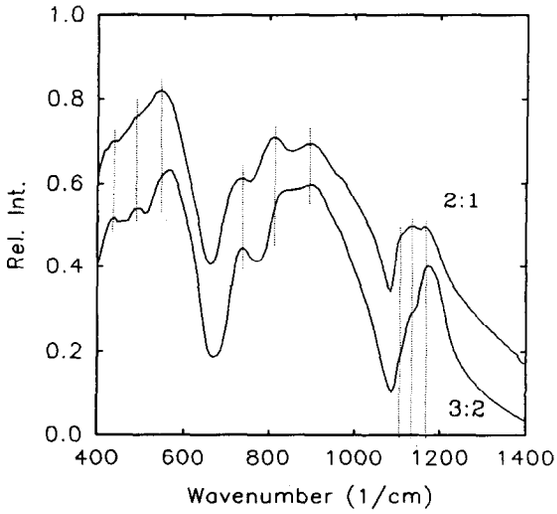

Fig. 1. IR absorption spectra of two mullites of known composition: $2Al_2O_3{\cdot}1SiO_2$ (2:1 mullite, $x = 0{\cdot}4$) and $3Al_2O_3{\cdot}2SiO_2$ (3:2 mullite, $x = 0{\cdot}25$). Dotted vertical lines are given as a guide for the eye, to enable comparison (see text). The spectra are shifted vertically for better comparison.

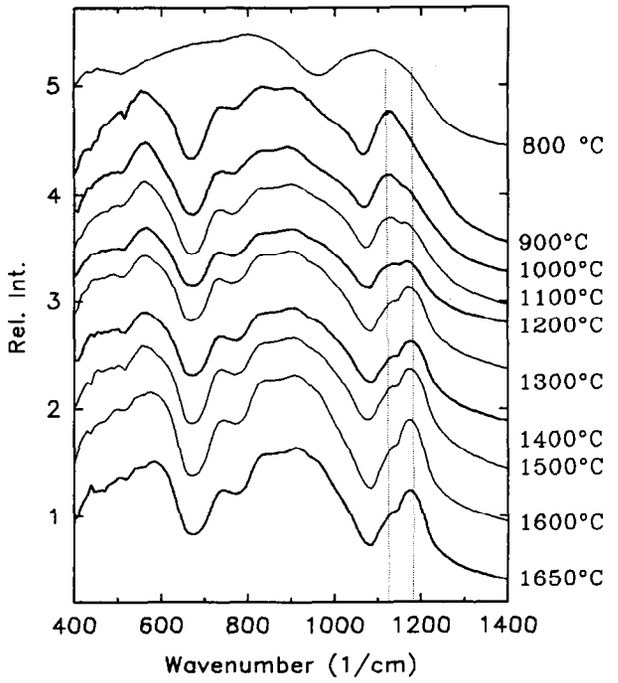

Fig. 2. IR absorption spectra of route of crystallization of type I precursor starting material with the burning temperatures as shown. The spectra are shifted vertically for better comparison. Dotted lines are a guide for the eye.

to a superposition of two peaks of high and low intensity, which were assigned to $[AlO_4]$ (1165 cm^{-1}) and $[SiO_4]$ (1125 cm^{-1}) species, respectively. In the spectra shown here, there are three positions marked that will be discussed further below.

The spectra observed for the route of crystallization of type I, II and III precursor starting materials are shown in Figs 2, 3 and 4, respectively. It has been shown earlier[5] that precursor starting material of type I shows a higher degree of homogeneity than types II and III, i.e. there are larger Al-rich clusters in the type II and III materials.

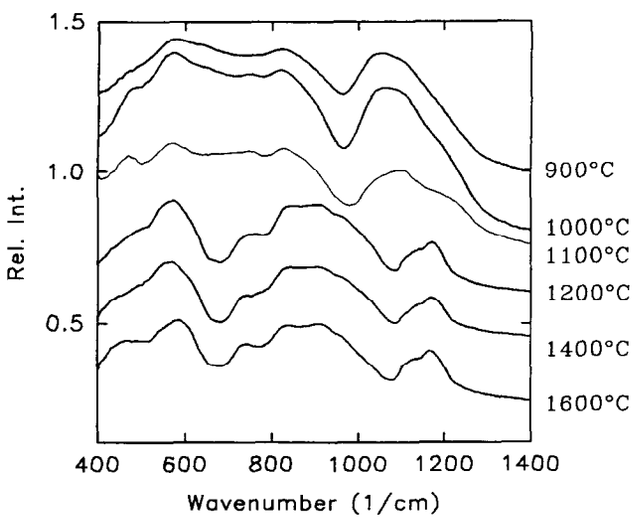

Fig. 3. IR absorption spectra of route of crystallization of type II precursor starting material with the burning temperatures as shown. The spectra are shifted vertically for better comparison.

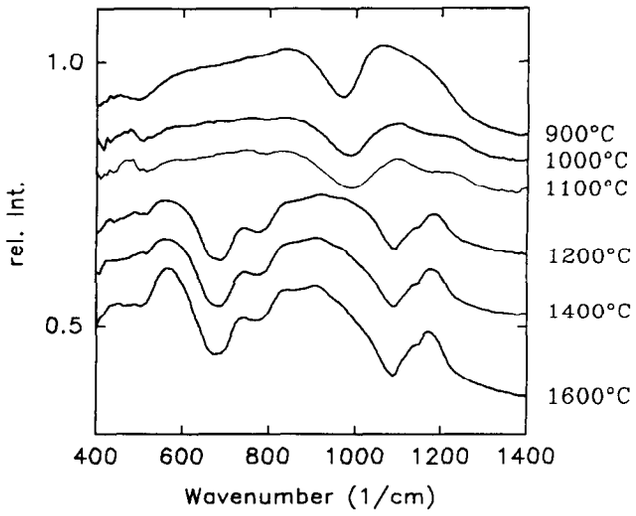

Fig. 4. IR absorption spectra of route of crystallization of type III precursor starting material with the burning temperatures as shown. The spectra are shifted vertically for better comparison.

Therefore, it can be understood that γ-Al_2O_3 crystallizes first[5] (compare also Ref. 8) in these cases. Inspection of the spectra in Figs 3, 4 and 1 shows that mullite crystallization is proved for the material burned at 1200°C without significant changes in the mullite spectra towards higher burning temperatures. These findings are in agreement with the X-ray results. The changes in the spectra for 900 to 1100°C may be related to prior crystallization (γ-Al_2O_3). In contrast to this, the infra-red absorption spectra show that the formation of mullite for type I precursor material has already occurred at 900°C, with, however, significant changes observed in the 1100 to 1200 cm^{-1} absorption profiles at higher firing temperatures. These changes are in close agreement with observations reported by Cameron[1] for mullites of different Al_2O_3 to SiO_2 ratios ($0{\cdot}6 < x < 0{\cdot}25$). It may be noted that the mullite spectra in Fig. 2 also show a systematic decrease of the intensity of the peak structures at 810 cm^{-1} relative to the one at 895 cm^{-1}, but these changes are too small to be followed in detail.

For a first rough determination of the evolution of the absorption profile in the spectral range 1100 to 1200 cm^{-1}, the intensities in the spectra of the series of samples of type I (Fig. 2) were measured at 1130 cm^{-1} and 1170 cm^{-1} relative to the baseline for zero intensity obtained at 2000 cm^{-1} (not shown; note that the spectra are shifted vertically for better comparison). The ratios of the intensities $I(1130\ cm^{-1})/I(1170\ cm^{-1})$ are shown in Fig. 5 as a function of the firing temperatures. Also indicated in this figure are the ratios obtained for the 2:1 and 3:1 mullites from Fig. 1. The systematic variation of the data implies that the composition of the mullite changes gradually from Al-rich mullite

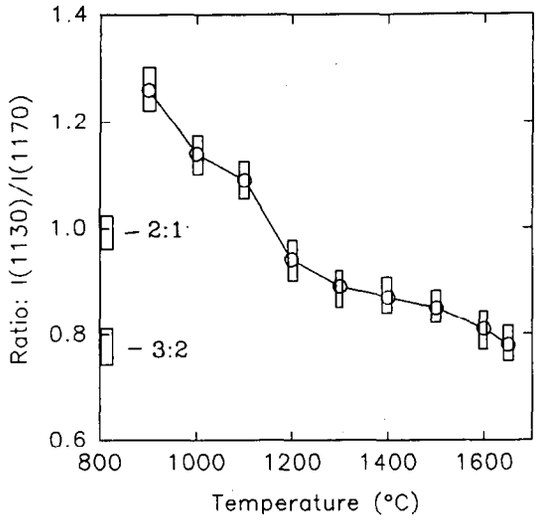

Fig. 5. Ratio of absorption measured at 1130 and 1170 cm^{-1} of the spectra given in Fig. 2 as a function of temperature. Values obtained for ideal 3:2 and 2:1 mullites (Fig. 1) are marked. Boxes indicate the experimental uncertainty. Solid line is a guide for the eye.

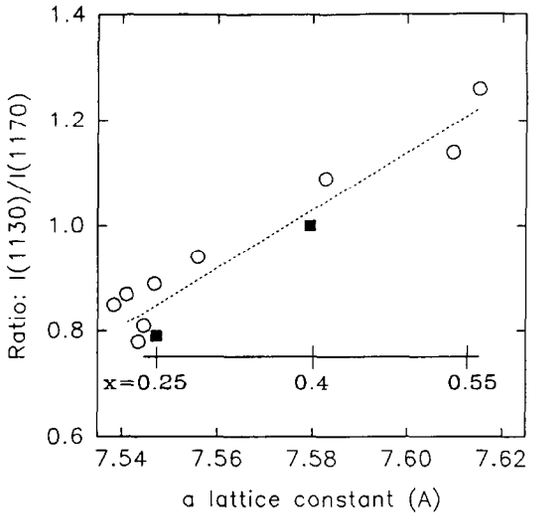

Fig. 7. Intensity ratio $I(1130cm^{-1})/I(1170cm^{-1})$ as a function of **a** lattice constants for mullites of composition 3:2 and 2:1 (black squares) and mullites obtained from the firing of type I precursors (open circles), with dotted line as a guide for the eye. Also shown is the linear scale of mullite compositions according to $Al_2(Al_{2+2x}Si_{2-2x})O_{10-x}$ related on the **a** lattice constants.

to bulk 3:2 mullite as a function of increasing temperature of the firing process. This suggestion is supported by the behaviour of the lattice parameters, which are shown in Fig. 6. Okada and Otsuka[7] also obtained a similar functional dependence of the lattice constants of so-called 'xerogel' starting materials. These authors were also able to prove the change in Al content of the various mullite products by analytical transmission electron microscopy investigations. A similar phenomenon was also reported by Brown *et al.*[12] in the kaolinite–mullite reaction path, using ^{29}Si and ^{27}Al solid-state nuclear magnetic resonance spectroscopy.

The composition of the mullite products obtained here can be determined by inspecting Fig. 7, in which the intensity ratios are plotted as a function of the **a** lattice parameter. Also shown is the x scale for the chemical composition $[Al_2(Al_{2+2x}Si_{2-2x})O_{10-x}]$ according to the linear relationship to the **a** lattice constant. It is of interest to note that this linear dependence holds irrespective of different ordering patterns of the oxygen vacancies,[13] providing a conclusive measure of the concentration of oxygen vacancies x. Thus, the IR data of the intensity ratio $I(1130)/I(1170)$ also imply a quasi linear relationship with the chemical composition of mullite. It may be noted that the absorption ratios $I(1130)/I(1170)$ for the mullite products of type II and III precursors (Figs 3 and 4) would indicate $x \approx 0{\cdot}25$, i.e. there is no change in composition as a function of firing temperature between 1200 and 1600°C.

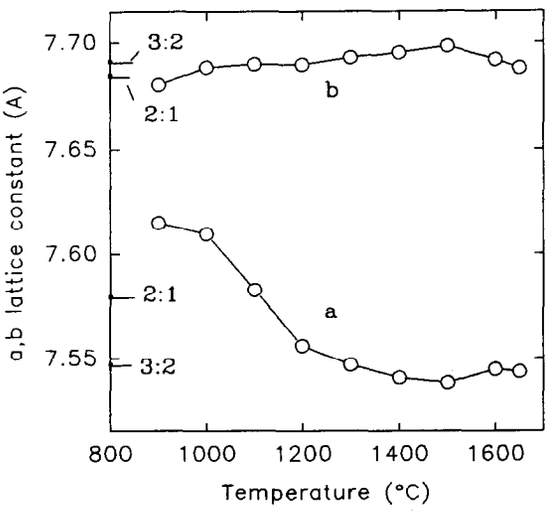

Fig. 6. Refined **a** and **b** lattice constants for the mullite sample according to the firing processes of type I precursors. (c = 2·888 ± 0·001 Å, not shown). **a** and **b** values for the mullites of composition 3:2 and 2:1 are marked by horizontal lines.

IR spectra of mullites in the field of nominal composition $x = 0$ to $x = 0{\cdot}7$ were also shown by Colomban.[4] Comparison of the 1100 to 1200 cm^{-1} absorption features to results presented here would tentatively indicate Si-rich mullite ($x < 0{\cdot}4$) in the presentation in Ref. 4. However, discrimination between mullites of various compositions from the 1100–1200 cm^{-1} absorption characteristics was not considered in that study and therefore will not be discussed further here.

4 Discussion

It has been shown above that the intensity ratio of the absorption $I(1130\ cm^{-1})/I(1170\ cm^{-1})$ follows an approximately linear relationship with the composition of mullite $Al_2(Al_{2+2x}Si_{2-2x})O_{10-x}$. Therefore this ratio might be used as an empirical scale for the determination of mullite compositions. Okada

and Otsuka[7] and Voll[9] (compare also Schneider *et al.*[3]) reported a discontinuous development of the compositional dependence of mullite as a function of the firing process for type I (homogeneous) precursors. These authors observed plateau-like behaviour of the **a** lattice constant (and some anomalies in the **b** and **c** parameters) for temperatures in the range 1000 to 1100°C. However, these features cannot be resolved from the present data and can be disregarded for the further discussion here.

Problems with the use of the empirical scale of the IR absorption in the range 1100 to 1200 cm^{-1} could be related to the coexistence of an amorphous (glassy) phase with the mullite crystals. This phase has to be considered in the crystallization route of the type I precursor, because SiO_2 or $(nSiO_2)\cdot(mAl_2O_3)$ glass phase is known to show an absorption peak in the spectral range 1000 to 1100 cm^{-1}. Thus, with the gradual formation of mullites with $x \approx 0{\cdot}55$ at 900°C to $x \approx 0{\cdot}25$ above 1300°C, the volume fraction of the residual amorphous phase should gradually decrease, which could be indicated by decrease of the absorption intensity observed at ~ 1130 cm^{-1} (Fig. 2). On the other hand, there are indications – at least for the formation of mullite from type I precursors above 1000°C – that the volume fractions of the amorphous state show less influence* than the mullite absorption cross-sections. This may be verified by inspecting the absorption profiles of pure phases of 3:2 and 2:1 mullite shown in Fig. 1 and comparing them with the various spectra in Fig. 2. Additionally, this conclusion is supported by the 1100 to 1200 cm^{-1} absorption spectra for pure mullite phases of different compositions reported by Cameron,[1] where the line profiles show a similar dependence as obtained in Fig. 2.

A deeper understanding of the changes in the absorption line profiles requires a detailed line profile analysis. This is not a simple task for powder-related spectra and anisotropic materials with a high number of atoms per unit cell, like mullite. With simple structural models ($[AlO_6]$, $[AlO_4]$ and $[SiO_4]$ units), MacKenzie[10] calculated the phonon frequencies of nine fundamental vibrations and related them to peak positions of the KBr powder spectra of a 3:2 mullite in the spectral range 400 to 1200 cm^{-1}. On the other hand, the number of IR active modes expected for the average structure of mullite ($4B_{1u}$, $9B_{2u}$, $9B_{3u}$;[11] compare also Ref. 14 from this issue) already indicates that the true number of IR active modes could largely be enhanced, compared with those resolved by the KBr experiment. The *average structure of mullite* (see, e.g., Refs 15 and 16) can most easily be understood by assuming an idealized half of the sillimanite unit cell ($c/2 \approx 2{\cdot}888$ Å) according to a statistical distribution of Al and Si on tetrahedral sites. Edge-sharing $[AlO_6]$ octahedra form chains, which run parallel to the z-axis. The centres of these octahedra are at (0,0,0) and (1/2,1/2,0). The oxygens of the (0 0 0) centred octahedra [on O_d sites $(x,y,0)$ and $(x,y,1)$] and one oxygen of the second octahedron [O_{ab} at $(x,y,1/2)$] form together with a fourth oxygen (O_c) at (0,1/2,1/2) or at (1/2,0,1/2) a tetrahedral unit, which is occupied by Si or Al (T_1 site). Thus, two T_1 tetrahedra always have a common O_c oxygen. The *real structure of mullite*, on the other hand, accommodates oxygen vacancies on the O_c sites, which are,

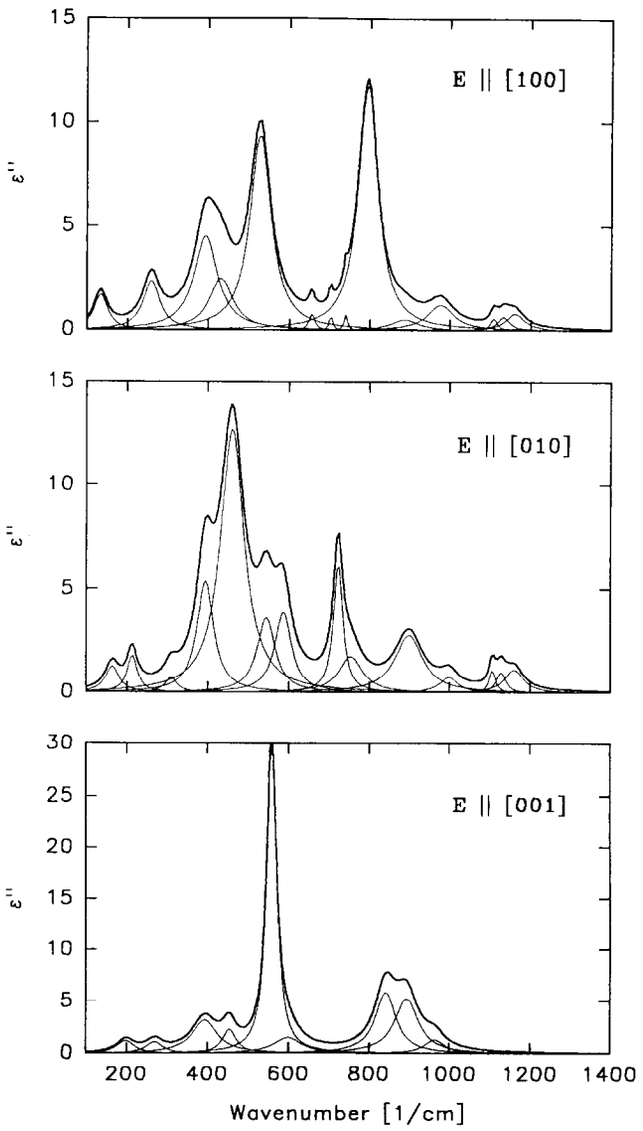

Fig. 8. Imaginary part of the dielectric function obtained by Kramers–Kronig transformation of the single crystal reflectivity of a 2:1 mullite (replotted from Ref. 11). Shown are the results of deconvolution into oscillator terms (thin lines) and their sum thick lines for the different polarizations.

*The contribution of the amorphous (glassy) phase to the IR absorption cross-section has still to be checked more accurately, e.g. by probing the cross-section of the pure phases.

therefore, fractionally occupied. Additionally, charge neutrality requires the substitution of $2Si^{4+} + O^{2-} = 2Al^{3+} + V$ (V = O_c vacancy). These aluminiums can be related to new Al* tetrahedral sites, creating O_c* oxygen sites, which are shifted from the O_c positions. Thus, Al*, O_c, O_c* and T_1 positions ought all to be fractionally occupied. By taking all atomic positions into account and assuming the rather hypothetical case of full occupation, the number of IR active modes are $13B_{3u}$, $13B_{2u}$ and $6B_{1u}$ according to polarizations parallel to the *a*, *b* and *c* lattice directions, respectively. For the sake of better comparison, the IR absorption spectra obtained from single crystal investigations of mullite of composition $x = 0{\cdot}4$ (2:1 mullite) are shown in Fig. 8 (for details see Ref. 11). The deconvolution of these spectra results in 14, 14 and 9 absorption bands with polarizations parallel to the [1 0 0], [0 1 0] and [0 0 1] lattice directions, respectively. According to this it can be concluded that the structural details of mullite result in a large number of modes, that are difficult to resolve in any detail from the KBr powder spectra (see Fig. 1), which sum over all directions of polarizations. However, the triplicate peak structure in the range 1100 to 1200 cm^{-1} can be separated and related back to the peaks in the B_{3u} and B_{2u} related spectra. For comparison, the KBr powder spectrum of 2:1 mullite and the summed single crystal absorption spectrum are shown in Fig. 9 (see also Fig. 1, where the three peak positions are marked). It may be noted that both spectra are in generally good agreement and that small discrepancies have to be related to the different measurement techniques.

Finally, it is interesting to get an assignment for the peak structure used to show the variation in the field of mullite of variable composition. MacKenzie[10] and Cameron[1] suggested only a duplicate peak structure in the spectral range 1100 to 1200 cm^{-1} in relation to $[AlO_4]$ and $[SiO_4]$ structural units. However, it is clear from the present study and from Ref. 11 that a third peak in this spectral range has to be taken into account for mullite, which might be assigned to an $[Al^*O_4]$ related tetrahedral vibration. According to this, the chemical variation of mullites $Al_2^{VI}(Al_2^{IV}Al_{2x}{}^*Si_{2-2x}^{IV})O_{10-x}$ should lead to a dependence of the intensity ratio $I(1108\ cm^{-1})/I(1165\ cm^{-1})$ as $2x/(2-2x)$, assuming no frequency shifts and no changes of absorption cross-section of each species as a function of x. Similarly, for the ratio $I(1130\ cm^{-1})/I(1165\ cm^{-1})$ a dependence according to $2/(2-2x)$ is expected, which increases more smoothly as a function of x than does the former. This increase seems to be justified by the observed dependence for the crystallization of type I precursors (see Fig. 7). However, for better information about this, the observed line profiles in the spectral range 1100 to 1200 cm^{-1} have to be deconvoluted quantitatively, which will be the task of further studies.

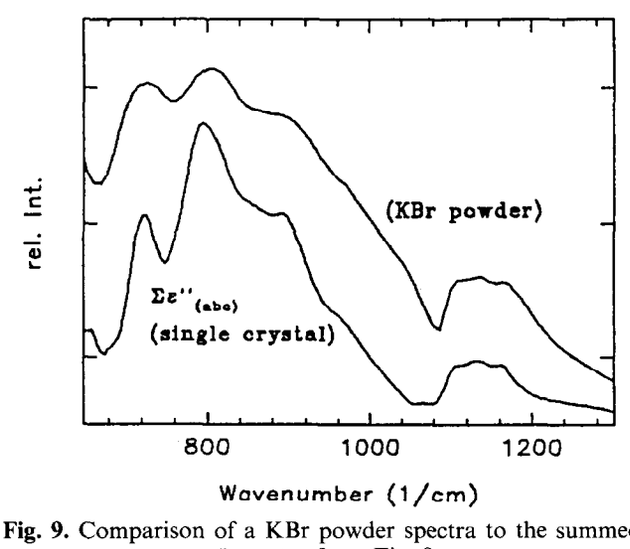

Fig. 9. Comparison of a KBr powder spectra to the summed ϵ'' spectra from Fig. 8.

Acknowledgements

The authors would like to express their thanks to Dr H. Schneider and co-workers (German Aerospace Establishment, Köln) for preparing the precursor starting materials for the present study. Professor E. Eberhard is gratefully acknowledged for his encouragement of this study and for many helpful discussions. Finally, we express our thanks to Professor K. J. D. MacKenzie for many helpful comments on the manuscript.

References

1. Cameron, W. E., Composition and cell dimensions of mullite. *Am. Ceram. Soc. Bull.*, **56** (1977) 1003–11.
2. Cameron, W. E., Mullite: a substituted alumina. *Am. Mineral.*, **62** (1977) 747–55.
3. Schneider, H., Okada, K. & Pask, J. A., *Mullite and Mullite Ceramics*, John Wiley and Sons, 1994, p. 31.
4. Colomban, Ph., Structure of oxide gels and glasses by infra-red and Raman scattering. *J. Mater. Sci.*, **24** (1989) 3011–20.
5. Schneider, H., Saruhan, B., Voll, D., Merwin, L. & Sebald, A., Mullite precursor phases. *J. Eur. Ceram. Soc.*, **11** (1993) 87–97.
6. Schneider, H., Voll, D., Saruhan, B., Sanz, J., Schrader, G., Rüscher, C. H. & Mosset, A., Synthesis and structural characterization of non-crystalline mullite precursors. *J. Non-Crystalline Solids*, 178 C19.
7. Okada, K. & Otsuka, N., Change in chemical composition of mullite formed from $2SiO_2{}^*3Al_2O_3$ xerogel during the formation process. *J. Am. Ceram. Soc.*, **70** (1987) C245–47.
8. Li, D. X. & Thomson, W. J., Tetragonal to othorhombic transformation during mullite formation. *J. Mater. Res.*, **6** (1991) 819–24.
9. Voll, D., Mullitprecursoren: Synthese, temperaturabhängige

Entwicklung der strukturellen Ordnung und Kristallisationsverhalten. Dr Thesis, University Hannover, 1994.
10. MacKenzie, K. J. D., Infrared frequency calculations for ideal mullite ($3Al_2O_3$*$2SiO_2$). *J. Am. Ceram. Soc.*, **55** (1972) 68–70.
11. Rüscher, C. H., Lattice vibrations of 2 : 1 mullite in infrared and Raman spectra. Submitted.
12. Brown, I. W. M., MacKenzie, K. J. D., Bowden, M. E. & Meinhold, R. H., Outstanding problems in the kaolinite–mullite reaction sequence investigated by ^{29}Si and ^{27}Al solid state nuclear magnetic resonance: II, high-temperature transformations of metakaolinite. *J. Am. Ceram. Soc.*, **68** (1985) 298–301.
13. Eberhard, E., Private communication, 1994.
14. Michel, D., Colomban, Ph., Abolhassani, S., Voyron, F. & Kahn-Harari, A., Germanium mullite: structure, phase relations and vibrational spectra of gels, glasses and ceramics. *J. Eur. Ceram. Soc.*, **16** (1996) 161–8.
15. Sadagana, R., Tokonami, M. & Takeuchi, Y., The structure of mullite, $2Al_2O_3$*SiO_2, and relationship with the structure of sillimanite and andalusite. *Acta Crystallogr.*, **15** (1962) 65–8.
16. Angel, R. J. & Prewitt, C. T., Crystal structure of mullite: a reeximation of the average structure. *Am. Mineral.*, **71** (1986) 1476–82.